PHYSICS AND CHEMISTRY OF SOLID STATE
V. 27, No. 2 (2026) pp. 391-398

Section: Physics

DOI: 10.15330/pcss.27.2.391-398

Vasyl Stefanyk Carpathian National University

ФІЗИКА І ХІМІЯ ТВЕРДОГО ТІЛА
Т. 27, № 2 (2026) С. 391-398

Фізико-математичні науки

UDC: 537.311.322

ISSN 1729-4428 (Print)
ISSN 2309-8589 (Online)

V.A. Romaka[1], Yu. Stadnyk[2], L. Romaka[2], A. Horyn[2], P. Demchenko[2], P. Haraniuk[1]

Features of mechanisms of electrical conductivity of semiconductor solid solution $Zr_{1-x}Al_xNiSn$

[1]*National University "Lvivska Politechnika", Lviv, Ukraine,* volodymyr.romaka@gmail.com;
[2]*Ivan Franko National University of Lviv, Lviv, Ukraine,* stadnykyu@gmail.com

The structural, electrokinetic, energetic, and magnetic properties of the semiconductor solid solution $Zr_{1-x}Al_xNiSn$, obtained by doping the half-Heusler phase *n*-ZrNiSn with Al atoms by substituting Zr atoms in the 4*a* position, were investigated. It was established that Al atoms can occupy different crystallographic positions, causing complex transformations of the crystal and electronic structures. It was shown that in $Zr_{1-x}Al_xNiSn$, $x = 0$–0.02, the increase in the unit cell parameter $a(x)$ is due to the preferential substitution of the Ni atoms present ($r_{Ni} = 0.125$ nm) in the 4*a* position by Al atoms ($r_{Al} = 0.143$ nm) generating defects and energy states of an acceptor nature. The decrease in the parameter $a(x)$ for $Zr_{1-x}Al_xNiSn$, $0.02 < x \leq 0.04$, is caused by the replacement of larger Zr atoms ($r_{Zr} = 0.160$ nm, $4d^25s^2$) with smaller Al atoms, which also generates defects and energy states of an acceptor nature. At concentrations of $Zr_{1-x}Al_xNiSn$, $x > 0.04$, Al atoms are mainly localized in tetrahedral voids of the structure, generating defects and energy states of a donor nature. The ratio of the concentrations of the generated energy states of $Zr_{1-x}Al_xNiSn$ determines the position of the Fermi level ε_F. The performed studies allowed us to identify the mechanisms of electrical conductivity to determine the conditions for the synthesis of thermoelectric materials $Zr_{1-x}Al_xNiSn$ with the maximum efficiency of converting thermal energy into electrical energy.

Keywords: semiconductor, electrical conductivity, thermopower coefficient, Fermi level.

Received 15 February 2026; Accepted 03 June 2026, Published 30 June 2026.

Introduction

The research results proposed for consideration continue the program of searching for new thermoelectric materials with maximum efficiency of converting thermal energy into electrical energy, in particular, the conditions for optimizing the electrokinetic properties of semiconductors based on half-Heusler phases *n*-*M*NiSn (*M* – Ti, Zr, Hf) (structure type MgAgAs, space group $F\bar{4}3m$ [1]) [2–4]. To obtain maximum values of the thermoelectric figure of merit Z ($Z=\alpha^2\cdot\sigma/\kappa$) by heavy doping the basic *n*-*M*NiSn semiconductors with donor and/or acceptor impurities, it is necessary to optimize the values of the thermopower coefficients α, the electrical conductivity σ, and the thermal conductivity coefficient κ [5].

In this context, it is interesting to study the semiconductor solid solution $Zr_{1-x}Al_xNiSn$, obtained by heavy doping of *n*-ZrNiSn with Al atoms ($3s^23p^1$), introduced into the structure by replacing Zr atoms ($4d^25s^2$) in the crystallographic position 4*a*. In this case, it is important to understand the entry mechanisms of Al atoms in the semiconductor matrix, in particular, the nature of the generated structural defects and the corresponding energy states. Such an understanding will allow for the building of a strategy for optimizing the electrokinetic properties of the thermoelectric material $Zr_{1-x}Al_xNiSn$ to obtain maximum values for the thermoelectric figure of merit Z [5]. Considering that the Zr atom contains more valence electrons than the Al atom, only structural defects of acceptor nature and the corresponding energy states were expected to be generated in the band gap ε_g of $Zr_{1-x}Al_xNiSn$. At the same time, doping the semiconductor *n*-ZrNiSn of the electronic conductivity type with an acceptor impurity Al will lead to an increase in the compensation degree due to the appearance and growth of the concentration of holes, as well as changes in the mechanisms of electrical

conductivity and even the type of main current carriers [6]. When studying the doping conditions with Al atoms of the half-Heusler phase *n*-TiNiSn, it was found that the impurity atoms occupy different crystallographic positions, simultaneously generating structural defects of donor and acceptor nature in different ratios [7].

Previous studies of the ZrNiSn compound have established peculiarities of its crystal and electronic structures [8]. It turned out that the structure of the ZrNiSn compound is disordered, and the crystallographic position 4*a* of Zr atoms is occupied by Ni atoms ($3d^84s^2$) to ~0.5%, which generates structural defects of a donor nature in the crystal (Ni has more *d*-electrons) and donor states in the band gap ε_g. Such a substitution of Zr atoms by Ni atoms implements the mechanism of "a priori doping" of the semiconductor with donors [9], and the formula of the ZrNiSn compound, taking into account the formed defects, can be expressed as $(Zr_{1-y}Ni_y)NiSn$, $y \leq 0{,}01$. Another feature of the structure of the ZrNiSn compound is the presence of tetrahedral voids, which constitute ~24% of the total volume of the unit cell and can be traps for both impurity and self-atoms of the compound, generating structural defects and corresponding energy states [8]. We deliberately focus on the features of the crystal structure of the ZrNiSn compound, since it is this knowledge that is the basis for understanding structural and energy transformations in the semiconductor solid solution $Zr_{1-x}Al_xNiSn$. The results of the study of the structural, electrokinetic, energy, and magnetic properties of the half-Heusler phase *n*-ZrNiSn doped with Al atoms presented below will allow us to identify the mechanisms of electrical conductivity to determine the conditions for the synthesis of thermoelectric materials with the maximum efficiency of converting thermal energy into electrical energy [5].

I. Research methods

$Zr_{1-x}Al_xNiSn$ samples, $x = 0.01$–0.10, were synthesized by arc-melting of the initial components in a purified argon atmosphere. To give the alloys an equilibrium state, homogenizing annealing was performed at a temperature of 1073 K for 700 h with subsequent quenching in cold water without prior breaking of the ampoules. *X*-ray phase and *X*-ray structural analyses were performed using diffraction data obtained on DRON-2.0m (Fe K_α-radiation) and STOE STADI P (Cu $K\alpha_1$ – radiation) diffractometers. The chemical composition of the samples was controlled by energy dispersive *X*-ray spectroscopy (Tescan Vega 3 LMU electron microscope). The structural parameters of $Zr_{1-x}Al_xNiSn$ samples were calculated using the Fullprof Suite program package [10]. For the ordered variant of the $Zr_{1-x}Al_xNiSn$ crystal structure by the KKR method in the approximation of the coherent potential CPA and the local density LDA for the exchange-correlation potential with the Moruzzi-Janak-Williams (MJW) parameterization [11], the distribution of the density of electronic states DOS [12] was calculated. The accuracy of the calculation of the Fermi level position is ε_F ±4 meV. Samples of the correct geometric shape were used to study the electrical transport properties. The temperature and concentration dependences of the electrical resistivity $\rho(T)$ and the thermopower coefficient $\alpha(T)$ of $Zr_{1-x}Al_xNiSn$ solid solution samples were measured in the ranges: $T = 80$–400 K, $N_{Al} = 1.9 \cdot 10^{20}$ см$^{-3}$ ($x = 0.01$) – $1.1 \cdot 10^{21}$ см$^{-3}$ ($x = 0.06$), and the specific magnetic susceptibility $\chi(x)$ (Faraday method) – at room temperature. The thermopower coefficient $\alpha(T)$ was measured by the potentiometric method (pure copper as a reference material). The voltage drop on the samples was determined for different directions of electric current to avoid the influence of a possible *p-n* junction at the contact points.

II. Study of crystal and electronic structure features of $Zr_{1-x}Al_xNiSn$

According to *X*-ray phase analysis, the powder patterns of the $Zr_{1-x}Al_xNiSn$ samples with Al content $x = 0$–0.06 were indexed in the structure type MgAgAs [1] and did not contain additional phases. In the ordered version of the crystal structure $Zr_{1-x}Al_xNiSn$, Zr(Al) atoms occupy the crystallographic position 4*a* (0, 0, 0), Ni – 4*d* (¼, ¼, ¼), Sn – 4*c* (½, ½, ½). Crystal structure refinements of the $Zr_{0.97}Al_{0.03}NiSn$ sample by the Rietveld method confirmed that it belongs to the structure type MgAgAs ($a = 0.61069(1)$ nm, $R_I = 0.0475$, $R_p = 0.0833$, $R_{wp} = 0.111$, $\chi^2 = 1.43$). The observed, calculated, and difference X-ray patterns of the $Zr_{0.97}Al_{0.03}NiSn$ sample are shown in Fig. 1*a*.

At higher concentrations of Al atoms in the $Zr_{1-x}Al_xNiSn$ samples, $x > 0.06$, insignificant reflections appeared in the powder patterns, which were identified as reflections belonging to the binary compounds $ZrSn_2$ and NiAl. For this reason, the study of the electrokinetic and magnetic properties of $Zr_{1-x}Al_xNiSn$ was carried out on samples with compositions $x = 0$–0.06, the powder patterns of which do not contain traces of additional phases.

Since the atomic radius of Al ($r_{Al} = 0.143$ nm) is smaller than the atomic radius of Zr ($r_{Zr} = 0.160$ nm), the modeling of the behavior of the unit cell parameter $a(x)$ of the $Zr_{1-x}Al_xNiSn$ samples showed as expected, a linear decrease in its values. At the same time, the calculation of the unit cell parameter $a(x)$ based on the obtained diffraction data showed that the entry of Al atoms into the crystal structure of the semiconductor is accompanied by complex structural transformations and not the expected linear change when replacing Zr atoms in the crystallographic position 4*a* (Fig. 1*b*). As seen from Fig. 1*b*, the introduction of the lowest concentration of Al atoms in the experiment, $x = 0.01$, is accompanied by an unexpected rapid increase in the unit cell parameter $a(x)$ of $Zr_{1-x}Al_xNiSn$. At the concentration of Al atoms, $x \approx 0.02$, the parameter $a(x)$ of the $Zr_{1-x}Al_xNiSn$ cell reaches maximum values, and at even higher concentrations, $x > 0.02$, the values $a(x)$ decrease.

In the Introduction, we focused on the features of the crystal structure of the ZrNiSn compound, which is disordered due to the substitution of some Zr atoms by Ni atoms in the crystallographic position 4*a* [8]. Since the atomic radius of Ni ($r_{Ni} = 0.125$ nm) is much smaller than the atomic radius of Al ($r_{Al} = 0.143$ nm), the increase in the unit cell parameter $a(x)$ of $Zr_{1-x}Al_xNiSn$ at

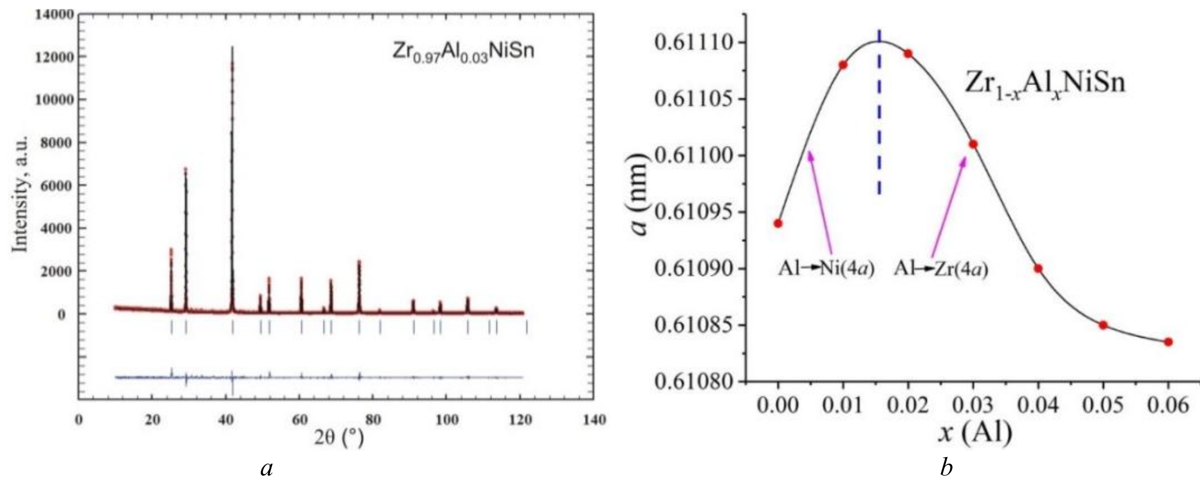

Fig. 1. X-ray patterns of $Zr_{0.97}Al_{0.03}NiSn$ sample (*a*) and variation of unit cell parameter $a(x)$ of semiconductor solid solution $Zr_{1-x}Al_xNiSn$ (*b*).

concentrations $0 < x \leq 0.02$ (Fig. 1b) is due to the substitution of Ni atoms ($3d^84s^2$) present there in the crystallographic position 4*a* by impurity Al atoms ($3s^23p^1$). Such a substitution is accompanied by generating structural defects of an acceptor nature in the $Zr_{1-x}Al_xNiSn$ crystal (the Al atom has fewer valence electrons than the Ni atom). In the band gap ε_g of the $Zr_{1-x}Al_xNiSn$ semiconductor, impurity acceptor states ε_A^1 will appear. At the same time, the same number of donor states ε_D that existed in *n*-ZrNiSn will disappear as a result of the substitution of Zr atoms ($4d^25s^2$) in position 4*a* by Ni atoms ("a priori doping" by donors [9]). The $Zr_{1-x}Al_xNiSn$ semiconductor becomes heavily doped and highly compensated [6].

As seen from Fig. 1*b*, the decrease in the unit cell parameter $a(x)$ of the $Zr_{1-x}Al_xNiSn$ in the concentration range $0.02 < x \leq 0.06$ is not linear, as it could be if the larger Zr atoms ($r_{Zr} = 0.160$ nm) were substituted by smaller Al atoms ($r_{Al} = 0.143$ nm) in the crystallographic position 4*a*. At the indicated concentrations, two parts can be conditionally distinguished in the $a(x)$ dependence: a rapid, practically linear decrease in the parameter in the range $0.02 < x \leq 0.04$ and a gentle change in the parameter reaching quasi-saturation at concentrations $x > 0.05$. We associate the rapid change in the parameter $a(x)$ of the $Zr_{1-x}Al_xNiSn$ at the concentration range $0.02 < x \leq 0.04$ with the substitution of Zr atoms by Al atoms in the 4*a* position.

At the same time, the $a(x)$ behavior of $Zr_{1-x}Al_xNiSn$ at concentrations $0.04<x$ is not obvious and cannot be explained by a simple substitution of some atoms by others. After all, in the $Zr_{1-x}Al_xNiSn$ structure, there is a linear increase in the concentration of Al atoms, and the rate of change of the parameter $a(x)$ decreases much more slowly and reaches quasi-saturation at $x > 0.05$. Below, based on the results of the electrokinetic and energetic properties of $Zr_{1-x}Al_xNiSn$, the mechanism of these structural changes, as well as changes in the electronic structure of the semiconductor, will be established.

The decrease in the unit cell parameter $a(x)$ of the $Zr_{1-x}Al_xNiSn$ solid solution in the concentration range $x > 0.02$ is understandable, and this is caused by the substitution in the crystallographic position 4*a* of larger Zr atoms ($r_{Zr} = 0.160$ nm) by smaller Al atoms ($r_{Al} = 0.143$ nm). In this case, such a substitution will generate defects of an acceptor nature in the crystal structure of $Zr_{1-x}Al_xNiSn$ since the Al atom ($3s^23p^1$) has fewer valence electrons than the Zr atom ($4d^25s^2$). At the same time, impurity acceptor states ε_A^2 of a different nature and depth of location also appear in the band gap ε_g of the semiconductor, which will increase the compensation degree. Since two different channels for generating acceptor states appear in an *n*-type semiconductor, at a certain concentration of Al atoms, a change in the type of main current carriers is possible.

Thus, X-ray structural studies of the semiconductor solid solution $Zr_{1-x}Al_xNiSn$ show that at different concentrations, Al atoms can displace Ni and Zr atoms from the crystallographic position 4*a*, generating structural defects of acceptor nature and the corresponding energy states. The ratio of donor and acceptor states of $Zr_{1-x}Al_xNiSn$ will determine the type of electrical conductivity (whether semiconductor or metallic), as well as the type of main current carriers. A similar effect was observed for the semiconductor solid solution $Ti_{1-x}Al_xNiSn$ [7].

To establish the Fermi level ε_F position relative to the continuous energy bands and the band gap width ε_g, the distribution of the density of electronic states (DOS) was calculated for the ordered variant of the crystal structure of the $Zr_{1-x}Al_xNiSn$ solid solution (Fig. 2). Since the

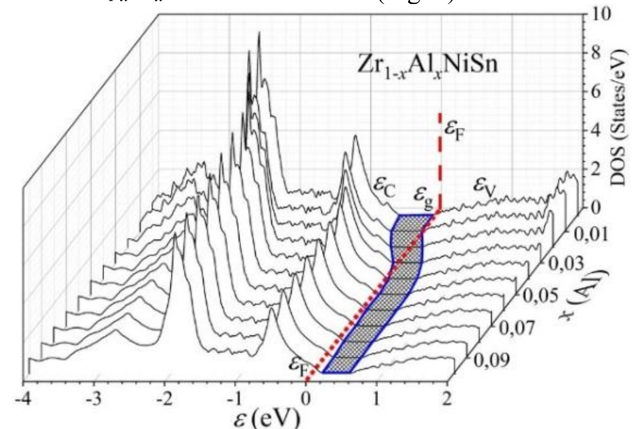

Fig. 2. Calculation of distribution of density of electronic states DOS for ordered variant of structure of semiconductor solid solution $Zr_{1-x}Al_xNiSn$.

substitution of Zr atoms by Al atoms in the crystallographic position 4*a* generates structural defects of an acceptor nature, even at the lowest concentration of Al atoms in the experiment, $x = 0.01$, the Fermi level ε_F (dashed line) begins to move away from the conduction band ε_C. At a concentration $x \approx 0.02$, the Fermi level ε_F will be located near the middle of the band gap ε_g of the semiconductor (full compensation state), which will cause the maximum values of the resistivity ρ in the experiment. At even higher concentrations, when the Fermi level ε_F crosses the middle of the band gap ε_g and approaches the valence band ε_V, the type of the main current carriers of the semiconductor will change. In the experiment, this will be reflected in positive values of the thermopower coefficients α, and holes will be the main current carriers of $Zr_{1-x}Al_xNiSn$. Calculations show that the Fermi level ε_F crossing of the valence band edge ε_V will occur at a concentration $x \approx 0.04$, which will change the type of electrical conductivity of $Zr_{1-x}Al_xNiSn$ from activation to metallic [6]. At the same time, activation parts will disappear in the temperature dependences of the resistivity $\ln(\rho(1/T))$ of $Zr_{1-x}Al_xNiSn$, and the increase in the electrical resistivity $\rho(T)$ with temperature will be caused by the mechanisms of scattering of current carriers. Electrokinetic studies of the $Zr_{1-x}Al_xNiSn$ solid solution will show the degree of adequacy of the results of modeling its electronic structure, as well as the conclusions of structural studies regarding the generation of only acceptor states in the semiconductor.

III. Study of electrokinetic, energetic and magnetic properties of $Zr_{1-x}Al_xNiSn$

Fig. 3 and 4 show the temperature and concentration dependences of the resistivity ρ and the thermopower coefficients α of the semiconductor solid solution $Zr_{1-x}Al_xNiSn$, x=0–0.06. The presence of high- and low-temperature activation parts on the $\ln(\rho(1/T,x))$ and $\alpha(1/T,x)$ dependences (Fig. 3) indicates that the studied samples are doped and compensated semiconductors, in which there are several activation mechanisms of electrical conductivity [6]. The temperature dependences $\ln(\rho(1/T,x))$ of $Zr_{1-x}Al_xNiSn$ can be described by formula (1) [6]:

$$\rho^{-1}(T) = \rho_1^{-1} exp\left(-\frac{\varepsilon_1^{\rho}}{k_B T}\right) + \rho_3^{-1} exp\left(-\frac{\varepsilon_3^{\rho}}{k_B T}\right), \qquad (1)$$

where the first high-temperature term describes the activation of current carriers $\varepsilon_1^{\rho}(x)$ from the Fermi level ε_F to the conduction band ε_C, and the second, low-

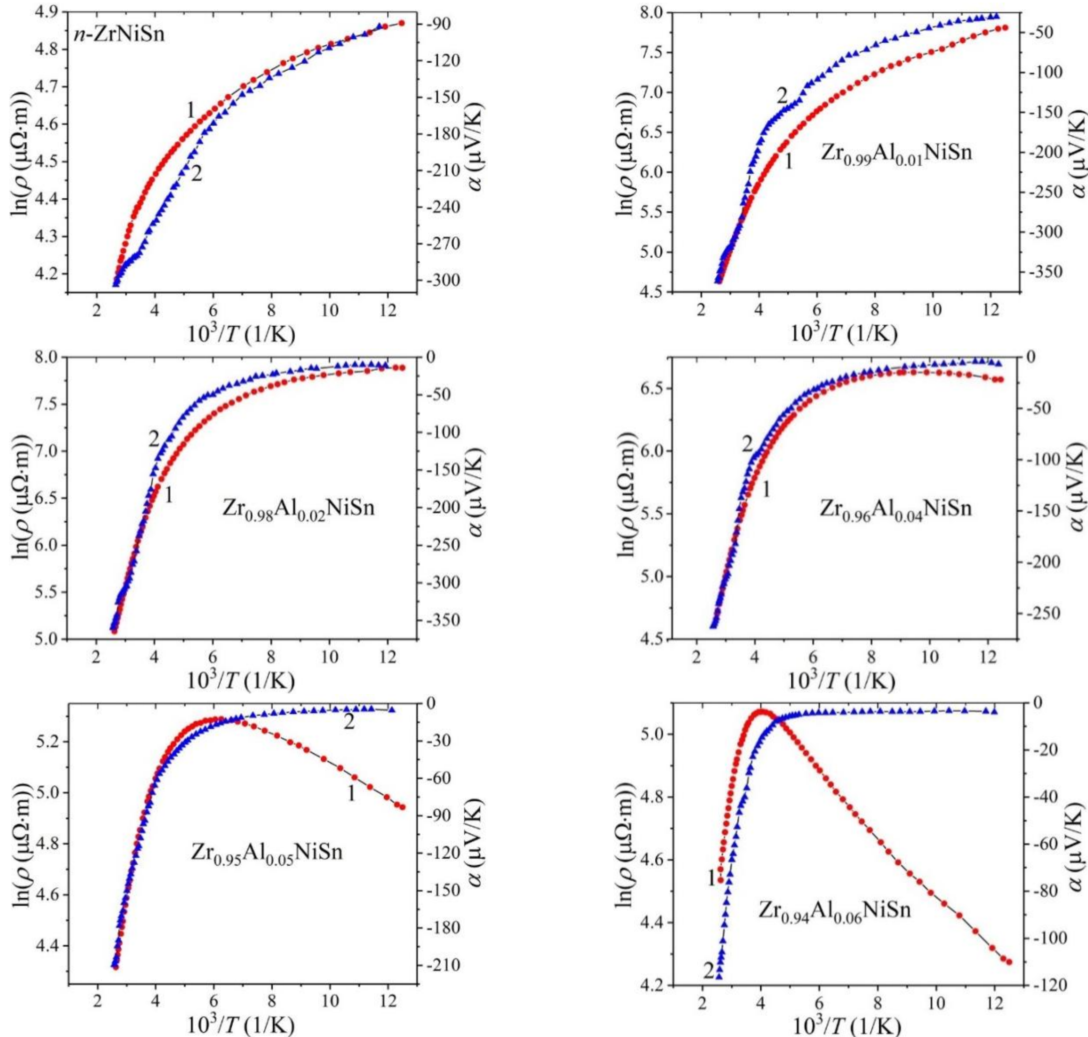

Fig. 3. Temperature dependences of resistivity $\ln(\rho(1/T,x))$ (1) and thermopower coefficient $\alpha(1/T,x)$ (2) of semiconductor solid solution $Zr_{1-x}Al_xNiSn$.

temperature term describes the jump conductivity $\varepsilon_3^{\rho}(x)$ with energies close to the Fermi level ε_F. The values of the activation energies $\varepsilon_1^{\rho}(x)$ from the Fermi level ε_F to the conduction band ε_C calculated by formula (1) are shown in Fig. 5*a*, curve 1.

The change in the thermopower coefficient $\alpha(1/T,x)$ $Zr_{1-x}Al_xNiSn$ (Fig. 3) with temperature is described by formula (2) [6]:

$$\alpha = \frac{k_B}{e}\left(\frac{\varepsilon_i^{\alpha}}{k_B T} - \gamma + 1\right), \qquad (2)$$

where γ is a parameter that depends on the nature of the scattering mechanisms. Based on formula (2), the activation energies $\varepsilon_1^{\alpha}(x)$ and $\varepsilon_3^{\alpha}(x)$ were calculated from the high- and low-temperature activation parts of the $\alpha(1/T,x)$ dependence. The authors [3, 4] showed that the energies $\varepsilon_1^{\alpha}(x)$ and $\varepsilon_3^{\alpha}(x)$ are proportional to the amplitude of the large-scale fluctuation of the continuous energy bands and the small-scale fluctuation of the doped and compensated semiconductor. The higher the degree of compensation of the semiconductor, the greater the amplitude of the band modulation [6]. The calculated values of the activation energy $\varepsilon_1^{\alpha}(x)$ of the semiconductor solid solution $Zr_{1-x}Al_xNiSn$ are displayed in Fig. 5*a* (curve 2).

The high-temperature activation observed in the $\ln(\rho(1/T,x))$ dependences of $Zr_{1-x}Al_xNiSn$ suggests that the Fermi level ε_F is located within the band gap ε_g of the semiconductor, close to the conduction band ε_C, indicating that electrons are the primary carriers of current. This is confirmed by the negative values of the thermopower coefficients $\alpha(1/T,x)$ at all concentrations and temperatures (Fig. 3, 4). While the experimental results of the change in the resistivity ρ and the thermopower coefficients α of $Zr_{1-x}Al_xNiSn$ with temperature at concentrations $x = 0$–0.02 are consistent with the results of modeling the electronic structure (Fig. 2), in the samples with an Al content of $0.02<x\leq0.06$ there are discrepancies. The first such discrepancy is the negative values of the thermopower coefficients α for the $Zr_{1-x}Al_xNiSn$ samples, $0.02<x\leq0.06$. This means that the Fermi level ε_F at all investigated concentrations of Al atoms remains in the band gap ε_g and lies closer to the conduction band ε_C than to the valence band ε_V. Even though the above-considered transformations of the crystal and electronic structures of $Zr_{1-x}Al_xNiSn$ predicted the appearance of only acceptor states and their growth with increasing concentration of Al atoms, the experiment also suggests the process of generating donor states by an unestablished mechanism that compensates for the acceptor states.

Analysis of the temperature dependences $\ln(\rho(1/T,x))$ for $Zr_{1-x}Al_xNiSn$ (Fig. 3) shows that in the samples ZrNiSn, $Zr_{0.99}Al_{0.01}NiSn$ and $Zr_{0.98}Al_{0.02}NiSn$ at low temperatures, the electrical conductivity is determined by

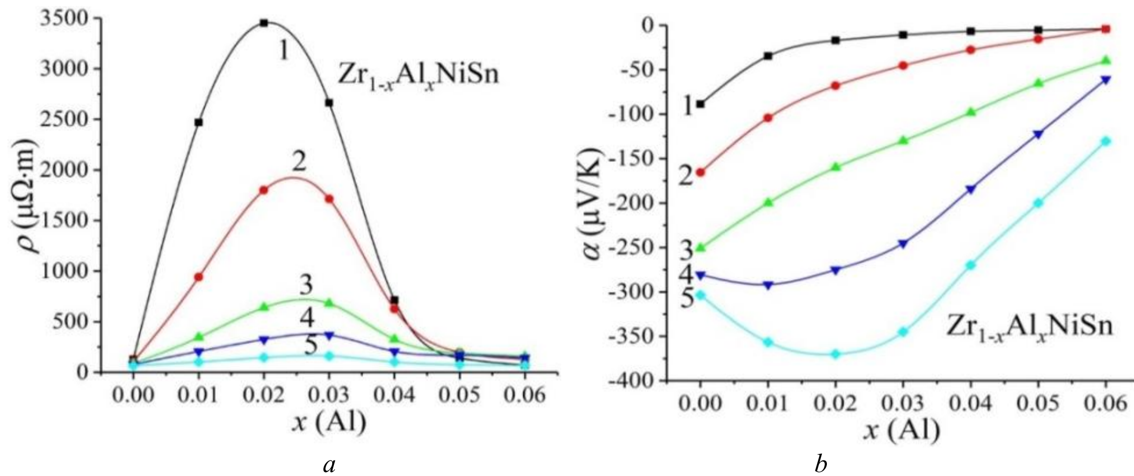

a *b*

Fig. 4. Change in resistivity $\rho(x,T)$ (*a*) and thermopower coefficient $\alpha(1/T,x)$ (b) of $Zr_{1-x}Al_xNiSn$ at different temperatures: 1 – T=80 K; 2 – T=160 K; 3 – T=250 K; *4* – T=300 K; 5 – T=380 K.

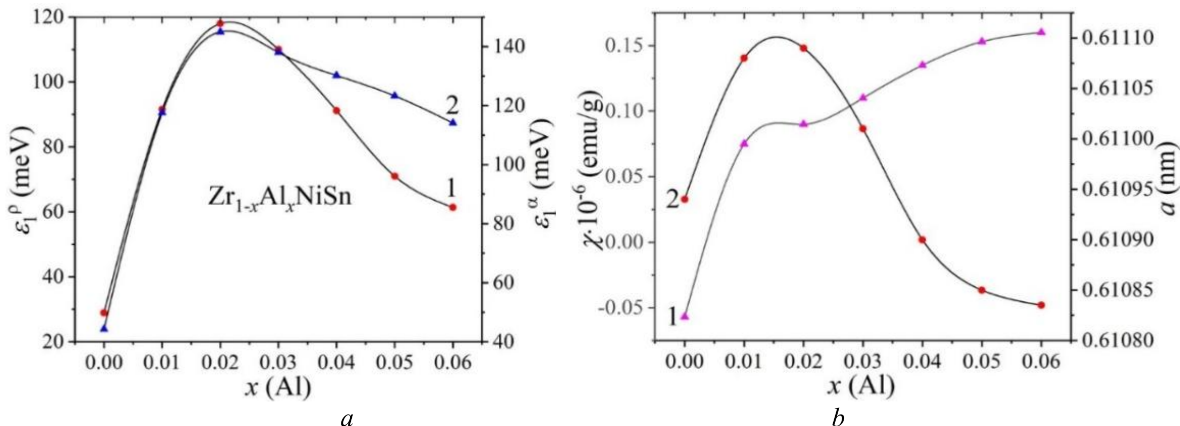

a *b*

Fig. 5. Change in activation energies ε_1^{ρ} (1) and ε_1^{α} (2) (*a*), specific magnetic susceptibility $\chi(x)$ (1) and unit cell parameter $a(x)$ (2) (*b*) of semiconductor solid solution $Zr_{1-x}Al_xNiSn$.

carrier jumps in localized states in the vicinity of the Fermi energy ε_F. The existence of jump ε_3^ρ-conductivity in *n*-type semiconductors at relatively small concentrations of acceptors is understandable. The absence of jump ε_3^ρ-conductivity at higher concentrations of acceptors $Zr_{1-x}Al_xNiSn$, x=0.03–0.06, when the sign of the thermopower coefficient α is negative, is not understandable. In these samples at low temperatures, the electrical resistivity values increase with rising temperature, indicating metallic conductivity. The metallization of low-temperature conductivity for $Zr_{1-x}Al_xNiSn$ samples, x=0.03–0.06, indicates the presence near the edge of the conduction band ε_C of a significant number of small donor states of unknown origin, the wave functions of which crossing the states of the conduction band ε_C and forming a "tail". Such energy proximity facilitates the ionization of donors and the appearance of a significant number of free electrons in the conduction band ε_C.

Thus, the experimental results indicate that in $Zr_{1-x}Al_xNiSn$ samples, x=0.03–0.06, at low temperatures, there is a significant number of donor states, the concentration of which exceeds the concentration of generated acceptor states. This is shown by negative values of the thermopower coefficient $\alpha(x,T)$ and metallic conductivity at low temperatures. In this case, the Fermi level ε_F is located in the band gap ε_g at a significant distance from the edge of the conduction band ε_C.

Doping *n*-ZrNiSn with the lowest concentration of Al atoms in the experiment at concentrations x = 0–0.02 is accompanied by an increase in the resistivity $\rho(x,T)$ for all studied temperatures, for example, at T = 80 K from $\rho_{x=0}$=129.1 μΩ·m to $\rho_{x=0.02}$=3450.3 μΩ·m and $\rho_{x=0.03}$=2663.4 μΩ·m·(Fig. 4*a*). At the same time, the values of the thermopower coefficient $\alpha(x,T)$ at these concentrations and studied temperatures remain negative, indicating the location of the Fermi level ε_F in the band gap ε_g near the conduction band ε_C (Fig. 4*b*). The change in the resistivity $\rho(x,T)$ and thermopower coefficient $\alpha(x,T)$ for $Zr_{1-x}Al_xNiSn$ at concentrations x = 0–0.02 is consistent with the conclusions of structural studies. Thus, when analyzing the structural transformations of $Zr_{1-x}Al_xNiSn$, it was found that the increase in the unit cell parameter $a(x)$ at concentrations x=0–0.02 is due to the substitution of Al atoms in the crystallographic position 4*a* for the Ni and Zr atoms present there, which generates acceptor states in the band gap ε_g.

At a concentration x≈0.02 and a temperature T = 80 K, an extremum appears on the dependences of the resistivity $\rho(x,T)$ of $Zr_{1-x}Al_xNiSn$, which shifts to the range of higher concentrations of Al atoms with increasing temperature. The appearance of the extremum on the dependence $\rho(x,T)$ is the result of a change in the ratio of ionized acceptor and donor states available in the semiconductor. In the *n*-type semiconductor $Zr_{1-x}Al_xNiSn$, a decrease in the resistivity $\rho(x,T)$ at concentrations of $0.2 < x \leq 0.06$ when doping, as expected, with an acceptor impurity is possible only in the case of the appearance and increase in the concentration of electrons of unknown origin.

In this context, a logical question arises regarding the mechanisms of donor generation in the $Zr_{1-x}Al_xNiSn$ semiconductor. The answer is related to the change of the electronic structure of $Zr_{1-x}Al_xNiSn$ due to of transformations in the crystal structure upon introducing Al atoms into the semiconductor matrix.

In the Introduction, it was noted that a feature of the structure of the ZrNiSn compound is the presence of tetrahedral voids, which constitute ~24% of the total volume of the unit cell. The authors [8] showed that for substitutional solid solutions based on the ZrNiSn compound, it is energetically expedient to occupy the tetrahedral voids of the structure with impurity atoms, as well as Ni atoms displaced from the crystallographic position 4*a*. In this case, structural defects of a donor nature and the corresponding energy states are generated in the semiconductor. We can assume that in the case of $Zr_{1-x}Al_xNiSn$ solid solution at concentrations of $x > 0.04$, Al atoms can also occupy the tetrahedral voids of the structure, generating donor states. What is important, such localization of impurity atoms must have practically no effect on the change in the unit cell parameter.

The assumption made regarding the occupation of tetrahedral voids of the $Zr_{1-x}Al_xNiSn$ structure by Al atoms and the generation of donor states is confirmed by the behavior of the unit cell parameter $a(x)$ at concentrations $x > 0.04$ (Fig. 1*b*). Since in the $Zr_{1-x}Al_xNiSn$ structure there is a linear increase in the concentration of Al atoms and the rate of decrease in the cell parameter is much slower, it is logical to conclude that some of the Al atoms are localized in the tetrahedral voids of the semiconductor structure. At the same time, as shown by the change in $a(x)$ for $Zr_{1-x}Al_xNiSn$ at x>0.04, increasing the concentration of Al atoms leads to a greater share of these atoms occupying the tetrahedral voids. This is indicated by the dependence of $a(x)$ on quasi-saturation at $x > 0.05$ (Fig. 1*b*).

The evidence of the generation of donor states when doping *n*-ZrNiSn with Al atoms is the behavior of the Fermi energy ε_F for $Zr_{1-x}Al_xNiSn$ at concentrations x = 0–0.06. Fig. 5*a* shows the change in the activation energy of electrons ε_1^ρ from the Fermi level ε_F to the conduction band ε_C (negative values of the thermopower coefficient $\alpha(x,T)$ (Fig. 3, 4*b*)). Doping *n*-ZrNiSn with Al atoms leads to a drift of the Fermi level ε_F from the conduction band ε_C to the middle of the band gap ε_g of $Zr_{1-x}Al_xNiSn$. Thus, if in *n*-ZrNiSn, the Fermi level ε_F was at a distance of 28.9 meV from the edge of the conduction band ε_C, then in the semiconductor $Zr_{0.99}Al_{0.01}NiSn$ it is already at a distance of 91.6 meV, and in $Zr_{0.98}Al_{0.02}NiSn$ – 118.2 meV. The drift of the Fermi level ε_F from the conduction band ε_C in an *n*-type semiconductor is possible only if the number of acceptor states increases, which corresponds to the results of structural studies and calculations of the electronic structure of $Zr_{1-x}Al_xNiSn$ (Fig. 2). However, at higher concentrations of Al atoms, the Fermi level ε_F, contrary to calculations, begins to move in the opposite direction to the conduction band ε_C, as evidenced by the negative values of the thermopower coefficient $\alpha(x,T)$ (Fig. 3, 4*b*). In particular, in the semiconductor $Zr_{0.97}Al_{0.03}NiSn$, the Fermi level ε_F is located at a distance of 110.1 meV from the conduction band ε_C, in $Zr_{0.96}Al_{0.04}NiSn$ at a distance of 91.2 meV, and in $Zr_{0.94}Al_{0.06}NiSn$ – 61.4 meV. The reverse movement of the Fermi level ε_F of $Zr_{1-x}Al_xNiSn$ at Al concentrations, $x > 0.02$, clearly indicates that a powerful source of donor states has appeared in the semiconductor, the generation

rate of which exceeds the generation rate of acceptor states.

Analysis of the behavior of the activation energy $\varepsilon_1^{\rho}(x)$ of $Zr_{1-x}Al_xNiSn$ shows that in the concentration range $x = 0$–0.02, the dependence is practically linear (Fig. 5*a*, curve 1). This allows us to estimate the motion rate of the Fermi level ε_F from the edge of the conduction band ε_C into the depth of the band gap ε_g, which is equal to $\Delta\varepsilon_F/\Delta x \approx 59.1$ meV/%Al. The reverse motion of the Fermi level ε_F in the concentration range $x = 0.03$–0.05 occurs with a rate ~3 times lower $\Delta\varepsilon_F/\Delta x \approx 19.5$ meV/%Al. The fact that in the two concentration ranges, the directions and the motion rates of the Fermi level ε_F are different indicates changes in the crystal and electronic structures of $Zr_{1-x}Al_xNiSn$, which are accompanied by different rates of generation of structural defects of acceptor and donor nature and their corresponding energy states. The results obtained do not allow us to derive numerical values of the generation rates of acceptor and donor states separately. This can only be done by comparing the results of experimental measurements of structural and energy properties with modeling these properties for various variants of atomic distribution in the cell nodes. However, this is beyond the scope of this work.

The presented results of changes in the structural (Fig. 1*b*), electrokinetic (Fig. 3, 4), and energy properties (Fig. 5*a*) of the $Zr_{1-x}Al_xNiSn$ solid solution are consistent with the results of experimental measurements of the magnetic susceptibility $\chi(x)$ (Fig. 5*b*). Measurements of the magnetic susceptibility $\chi(x)$ of $Zr_{1-x}Al_xNiSn$ confirmed the previous results for the *n*-ZrNiSn semiconductor [3, 4, 8], which is a weak diamagnet. This is indicated by the negative values of the magnetic susceptibility $\chi = -0.07\cdot10\text{-}6$ cm^3/g as seen from Fig. 5*b*. At the lowest concentration of Al atoms in the experiment, $x = 0.01$, the magnetic state of the $Zr_{1-x}Al_xNiSn$ semiconductor changes, which becomes a Pauli paramagnet. Since the specific magnetic susceptibility of a Pauli paramagnet is determined exclusively by the electron gas and is proportional to the density of states at the Fermi level $g(\varepsilon_F)(x)$, the increase in the values of $\chi(x)$ at concentrations of Al atoms, $0.02<x$, is the result of an increase in the concentration of free electrons according to the mechanism described above.

Thus, studies of the electrokinetic, energetic, and magnetic properties of the semiconductor solid solution $Zr_{1-x}Al_xNiSn$, $x = 0$–0.06, not only confirmed the conclusions of structural studies regarding the substitution of Al atoms, depending on their concentration, of Zr and Ni atoms at position 4*a*, but also revealed the mechanism generating of donor states when Al atoms are localized in tetrahedral voids of the structure. This allowed us to identify the mechanisms of electrical conductivity to determine the conditions for synthesizing the thermoelectric material $Zr_{1-x}Al_xNiSn$ with the maximum efficiency of converting thermal energy into electrical energy.

Conclusions

The results of the study of the structural, electrokinetic, energetic, and magnetic properties of the new semiconductor solid solution $Zr_{1-x}Al_xNiSn$, obtained by doping *n*-ZrNiSn with Al atoms by substituting Zr atoms in the 4*a* position, revealed a complex nature of structural and energetic transformations. It was established that Al atoms can occupy different crystallographic positions, causing changes in the crystal and electronic structures. It was shown that in $Zr_{1-x}Al_xNiSn$, $x = 0$–0.02, the increase in the unit cell parameter $a(x)$ is due to the preferential substitution of Al atoms ($r_{Al} = 0.143$ nm, $3s^2 3p^1$) of the Ni atoms present there ($r_{Ni} = 0.125$ nm, $3d^8 4s^2$) in the 4*a* position, generating defects and energy states of an acceptor nature. The decrease in the parameter $a(x)$ of $Zr_{1-x}Al_xNiSn$, $0.02 < x \leq 0.04$, is caused by the replacement of larger Zr atoms ($r_{Zr} = 0.160$ nm, $4d^2 5s^2$) with smaller Al atoms, which also generates defects and energy states of an acceptor nature. At concentrations $x > 0.04$, Al atoms are mainly localized in tetrahedral voids of the structure, generating defects and energy states of a donor nature. The ratio of the concentrations of the generated energy states of $Zr_{1-x}Al_xNiSn$ determines the position of the Fermi level ε_F. The carried-out studies allowed us to identify the mechanisms of electrical conductivity for optimizing the synthesis parameters of thermoelectric materials $Zr_{1-x}Al_xNiSn$ with maximum efficiency of converting thermal energy into electrical energy.

Acknowledgments

The work was carried out within the framework of the Ministry of Education of Ukraine (grants № 0124U000989 and № 0124U001146).

Romaka Volodymyr – Proffesor of National University "Lvivska Politechnika";
Stadnyk Yuriy – Ph.D., Senior Scientist of Ivan Franko National University of Lviv;
Romaka Lyubov – Ph.D., Senior Scientist of Ivan Franko National University of Lviv;
Horyn Andriy **–** Ph.D., Senior Scientist of Ivan Franko National University of Lviv;
Demchenko Pavlo – Ph.D., Senior Scientist of Ivan Franko National University of Lviv;
Haraniuk Petro **–** docent of National University "Lvivska Politechnika".

[1] R. Marazza, R. Ferro, G. Rambaldi, *Some phases in ternary alloys of titanium, zirconium, and hafnium, with a MgAgAs or AlCu₂Mn type structure*, J. Less-Common Met., 39, 341 (1975); https://doi.org/10.1016/0022-5088(75)90207-6.

[2] V.A. Romaka, Yu.V. Stadnyk, V.Ya. Krayovskyy, L.P. Romaka, O.P. Guk, V.V. Romaka, M.M. Mykyychuk, A.M. Horyn, *The latest heat-sensitive materials and temperature transducers,* Lviv Polytechnic Publishing House, Lviv (2020); https://opac.lpnu.ua/bib/1131184.

[3] V.A. Romaka, M.G. Shelyapina, Yu.K. Gorelenko, D. Fruchart, Yu.V. Stadnyk, L.P. Romaka, V.F. Chekurin, *Special Features of Conductivity Mechanisms in Heavily Doped n-ZrNiSn Intermetallic Semiconductors*, Semiconductors, 40(6), 655 (2006); https://doi.org/10.1134/S10637826060608X.

[4] V.A. Romaka, Yu.V. Stadnyk, V.V. Romaka, D. Fruchart, Yu.K. Gorelenko, V.F. Chekurin, A.M. Horyn, *Features of electrical conductivity in the n-ZrNiSn intermetallic semiconductor heavily doped with the In acceptor impurity*, Semiconductors, 41(9) 1041 (2007); https://doi.org/10.1134/S1063782607090072.

[5] L.I. Anatychuk. Thermoelectricity. Physics of thermoelectricity, Institute of Thermoelectricity, Kyiv, Chernivtsi, Vol. 1 (1998).

[6] B.I. Shklovskii and A.L. Efros, *Electronic properties of doped semiconductors*, Springer-Verlag, Berlin, Heidelberg (1984); https://doi.org/10.1007/978-3-662-02403-4.

[7] Yu. Stadnyk, V.A. Romaka, L. Romaka, A. Horyn, V. Pashkevych, *Experimental studies of a new thermoelectric material based on semiconductor solid solution* $Ti_{1-x}Al_xNiSn$, Physics and chemistry of solid state, 25(1), 157 (2024). https://doi.org/10.15330/pcss.25.1.157-163.

[8] V.V. Romaka, P. Rogl, L. Romaka, Yu. Stadnyk, A. Grytsiv, O. Lakh, V. Krayovskii, *Peculiarities of structural disorder in Zr- and Hf-containing Heusler and half-Heusler stannides,* Intermetallics, 35, 45 (2013); http://dx.doi.org/10.1016/j.intermet.2012.11.022.

[9] V.A. Romaka, Yu.V. Stadnyk, L.G. Akselrud, V.V. Romaka, D. Fruchart, P. Rogl, V.N. Davydov, Yu.K. Gorelenko, *Mechanism of Local Amorphization of a Heavily Doped* $Ti_{1-x}V_xCoSb$ *Intermetallic Semiconductor*, Semiconductors, 42(7), 753 (2008); https://doi.org/10.1134/S1063782608070014.

[10] T. Roisnel, J. Rodriguez-Carvajal, *WinPLOTR: a windows tool for powder diffraction patterns analysis*. Mater. Sci. Forum, Proc. EPDIC7 378 (2001); https://doi.org/10.4028/www.scientific.net/MSF.378-381.118.

[11] V. Moruzzi, J. Janak, A. Williams, *Calculated Electronic Properties of Metals*, Pergamon Press, NY (1978). https://doi.org/10.1016/B978-0-08-022705-4.50002-8.

[12] M. Schruter, H. Ebert, H. Akai, P. Entel, E. Hoffmann, G.G. Reddy, *First-principles investigations of atomic disorder effects on magnetic and structural instabilities in transition-metal alloys*, Phys. Rev. B 52, 188 (1995); https://doi.org/10.1103/PhysRevB.52.188.

В.А. Ромака[1], Ю. Стадник[2], Л. Ромака[2], А. Горинь[2], П. Демченко[2], П. Гаранюк[1]

Особливості механізмів електропровідності напівпровідникового твердого розчину $Zr_{1-x}Al_xNiSn$

[1]*Національний університет "Львівська політехніка", Львів, Україна,* volodymyr.romaka@gmail.com;
[2]*Львівський національний університет ім. І. Франка, Львів, Україна,* stadnykyu@gmail.com

Досліджено структурні, кінетичні, енергетичні та магнітні властивості напівпровідникового твердого розчину $Zr_{1-x}Al_xNiSn$, отриманого легуванням фази пів-Гейслера *n*-ZrNiSn атомами Al шляхом заміщення у позиції 4*a* атомів Zr. Встановлено, що атоми Al можуть займати різні кристалографічні позиції, спричиняючи складні трансформації кристалічної та електронної структур. Показано, що в $Zr_{1-x}Al_xNiSn$, $x = 0$–0.02, ріст періоду елементарної комірки $a(x)$ зумовлений переважним заміщенням у позиції 4*a* атомами Al ($r_{Al} = 0.143$ нм, $3s^23p^1$) присутніх там атомів Ni ($r_{Ni} = 0.125$ нм, $3d^84s^2$), генеруючи дефекти та енергетичні стани акцепторної природи. Зменшення періоду $a(x)$ $Zr_{1-x}Al_xNiSn$, $0.02 < x \leq 0.04$, викликане заміщенням атомів більшого розміру Zr ($r_{Zr} = 0.160$ нм, $4d^25s^2$) меншими атомами Al, що також генерує дефекти та енергетичні стани акцепторної природи. За концентрацій $Zr_{1-x}Al_xNiSn$, $x > 0.04$, атоми Al переважно локалізуються у тетраедричних пустотах структури, генеруючи дефекти та енергетичні стани донорної природи. Співвідношення концентрацій генерованих енергетичних станів $Zr_{1-x}Al_xNiSn$ визначає положення рівня Фермі ε_F. Проведені дослідження дозволили ідентифікувати механізми електропровідності для визначення умов синтезу термоелектричних матеріалів $Zr_{1-x}Al_xNiSn$ з максимальною ефективністю перетворення теплової енергії в електричну.

Ключові слова: напівпровідник, електропровідність, коефіцієнт термо-ерс, рівень Фермі.